



Short communication

Superhydrophobic and high adhesive performance of functionalized graphene films

Yang Zhou ^{a,1}, Fengming Xu ^{a,1}, Guohua Jiang ^{a,b,*}, Xiaohong Wang ^{a,b}, Ruanbing Hu ^{a,b}, Rijiang Wang ^{a,b}, Xiaoguang Xi ^{a,b}, Sheng Wang ^{a,b}, Tao Wang ^{a,b}, Wenxing Chen ^{a,b}

^a Department of Materials Engineering, College of Materials and Textile, Zhejiang Sci-Tech University, Hangzhou 310018, PR China

^b Key Laboratory of Advanced Textile Materials and Manufacturing Technology (ATMT), Ministry of Education, Zhejiang Sci-Tech University, Hangzhou 310018, PR China

ARTICLE INFO

Article history:

Received 17 May 2012

Received in revised form 10 July 2012

Accepted 15 July 2012

Available online 21 July 2012

Keywords:

Superhydrophobic
Adhesive performance
Graphene
Film

ABSTRACT

Graphene films with high hydrophobic and adhesive performance were fabricated via chemical modification of graphite oxide and heat reduction processes. Irregularly stacked multilayer graphene nanosheets comprised the microstructure, whereas folding and agglomeration of graphene nanoflakes with few layers comprised the nanostructure. The resulting films showed remarkable superhydrophobic property with a static contact angle of 160.5°. Unlike many superhydrophobic materials, the obtained film is highly adhesive, allowing water drops as large as 50 μL to be inverted. Meanwhile, the film can be absolutely wet by silicone oil. This highly hydrophobic, oleophilic and adhesive performance of the graphene films could be useful in the device and biomaterial application.

© 2012 Elsevier B.V. All rights reserved.

1. Introduction

Carbon materials such as carbon nanotubes (CNTs) and graphene are some of the most promising materials for the incorporation of special functions into thin films, including mechanical applications and applications in catalysis and membranes [1,2]. Among the various possible applications of carbon materials already reported, surface wettability conversion is one of the most important application areas because of the unique physical properties required. In general, the wettability of a solid surface is strongly influenced both by its chemical composition and by its geometric structure (or surface roughness) [3].

Graphene is an ideal two-dimensional material with higher specific surface area than carbon nanofibers (CNFs) or CNTs, which is suitable for the formation of microscale surface roughness for a hydrophobic surface [4–6]. Several experimental and modeling studies have focused on exploiting surface roughness to engineer superhydrophobicity or superhydrophilicity. For example, Leenaerts et al. indicated that graphene is strongly hydrophobic based on density functional theory [7]. They concluded that the binding energies between water molecules are larger than the associated adsorption energies on the graphene surface, such that water molecules form clusters on the graphene sheet [7]. Yang et al. [8] reported that epitaxial graphene has a static contact angle (CA) of 92° and is slightly hydrophobic regardless of its thickness, whereas reduced graphene has a CA of 127° and a small interfacial

energy with water, regarding film structure. The roughening effect of the micro-/nanostructure on the graphene film surface greatly contributed to the wettability which could be controlled by UV irradiation and air storage [9]. Koratkar et al. reported that the surface roughness can be tuned by changing the solvent composition, which produces graphene films ranging from superhydrophobic to superhydrophilic [10].

In this study, we report a feasible method to produce superhydrophobic and functionalized graphene composite films with nano-scaled surface roughness. The graphene composite films were fabricated via three steps: chemical exfoliation of natural flake graphite following redox, functionalizing graphite oxide (GO) with (heptadecafluoro-1,1,2,2-tetradecyl) trimethoxysilane (HFTMS) and heat treatment of functionalized graphene composite films to create superhydrophobic surface. HFTMS has a long fluorocarbon chain, which will lower the surface energy of HFTMS-functionalized GO (GO-F). The GO-F film exhibits an enhanced surface roughness, which is essential for its superhydrophobicity.

2. Experimental

2.1. Materials

Graphite powder (40 μm) was obtained from Qingdao Henglide Graphite Co., Ltd. Concentrated sulfuric acid (H_2SO_4 , 98%), potassium permanganate (KMnO_4) and sodium nitrate (NaNO_3) were purchased from Shanghai Reagents Company and used as received. (Heptadecafluoro-1,1,2,2-tetradecyl) trimethoxysilane (HFTMS) were obtained from Hangzhou Feidian Chemical Co. Ltd. (Hangzhou, Zhejiang, China).

* Corresponding author at: Department of Materials Engineering, College of Materials and Textile, Zhejiang Sci-Tech University, Hangzhou 310018, PR China. Tel.: +86 571 86843527.

E-mail address: polymer_jiang@hotmail.com (G. Jiang).

¹ These authors contributed equally to this research work.

2.2. Preparation of GO

GO was synthesized through graphite powder oxidation with sulfuric acid and potassium permanganate ($\text{H}_2\text{SO}_4\text{-KMnO}_4$) [11].

2.3. Functionalization of GO and preparation of GO-F films

100 mg of GO was dispersed in 100 mL of ethanol containing 400 mg of HFTMS. The suspension was sonicated for 2 h. The HFTMS-GO was separated by filtration using a nylon membrane (0.02 μm , Whatman) and finally washed with ethanol to remove the excess HFTMS. The obtained HFTMS-GO was dried in vacuum at 60 °C for 24 h. The resulting solid was dispersed into ethanol under ultrasonic processing again to produce a supernatant solution. The supernatant solution was used to produce a thin film by a drop coating method and heat treatment processes. The resulting film was used for the measurement of the water contact angle (WCA).

2.4. Characterizations

The FT-IR characterizations were performed at ambient temperature with a spectrometer (Nicolet, Magna IR 560), which is equipped with diffuse reflectance accessories. Powder X-ray diffraction (XRD) analysis was analyzed by using X-ray diffractometer (i.e. SIEMENS Diffraktometer D5000, Germany) using $\text{Cu K}\alpha$ radiation source at 35 kV, with a scan rate of 0.02°. Thermogravimetric analysis (TGA) was measured on a thermogravimetric analyzer (TGA-2050, TA Instruments). Samples were heated at a rate of 20 °C/min in an ambient atmosphere. Water contact angle measurements were performed at ambient conditions using a Rame-Hart goniometer with a charge-coupled device camera equipped for image capture. Scanning electron microscopy (SEM) (LEO 1550) was used to investigate the surface morphology under an accelerating voltage of 4 kV.

3. Results and discussion

The structure and properties of GO depend on particular synthesis method and degree of oxidation. It typically preserves the layer structure of the parent graphite, but the layers are buckled and the interlayer spacing is about two times larger (~0.7 nm) than that of graphite [12,13]. GO is a nonstoichiometric material with lots of oxygen containing functional groups dispersed both in the basal plane and along the edges. The chemical structure of GO has been extensively studied but still controversial. It is generally agreed that the hydroxyl and epoxy groups are major functionalities that mainly exist in the basal plane with other functional groups located at the edges, including carbonyl ($=\text{CO}$), hydroxyl ($-\text{OH}$) and phenol groups [14,15]. These oxygen-containing functional groups make the GO hydrophilic with a surface free energy of 62.1 mJ/m^2 [16]. In order to decrease the surface energy of GO and turn it into hydrophobic, a fluorocarbon chain coupling agent, HFTMS was selected to chemically modify the GO. After functionalization, long fluorocarbon chains are exposed instead of hydrophilic functionalities on GO sheets. Materials with perfluoroalkyl chains are well known for their low surface energy and so high liquid repellency characteristics. Surface with regularly aligned closely packed CF_3 groups exhibited lowest surface energy of 6.7 mJ/m^2 well below the 18 mJ/m^2 value for poly(tetrafluoroethylene) [17]. Therefore, the GO-F is expected to have a similar surface energy to HFTMS, which is lower than that for graphite, 54.8 mJ/m^2 ; GO, 62.1 mJ/m^2 ; and graphene, 46.7 mJ/m^2 [16].

A schematic description of the process is shown in Scheme 1. The interaction between GO and HFTMS has three possibilities: hydrolysis between the alkoxy groups of HFTMS and hydroxyl groups of GO, hydrogen bonding, and nucleophilic substitution between epoxy and alkoxy. In most cases the silane is subjected to hydrolysis prior to the surface treatment. Following hydrolysis, a reactive silanol group

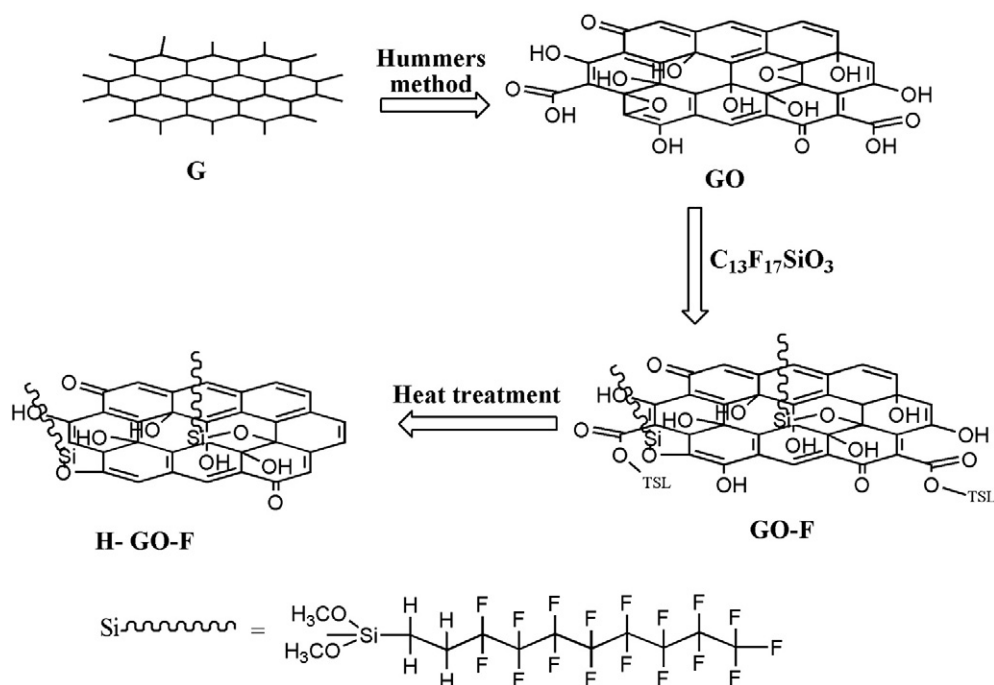
is formed, which can condense with other silanol groups to form siloxane linkages. It was also found that the silanol group opened the epoxy ring upon heating, concurrently with the silanol condensation [18]. Although the graphene films have been treated by heating, few carboxylate groups from the GO's layers and silanol groups still are present in the films. Hydrogen-bonding interactions may be formed between the carboxylate groups of the GO's layers and the oxygen-containing groups of guest molecules [19].

The FT-IR spectra of pristine graphite (G), graphite oxide (GO), HFTMS modified GO (GO-F) and GO-F after heat treatment (H-GO-F), as shown in Fig. 1, give information on the chemical reactions in the different functionalization steps. In the spectrum of G, no characteristic peaks can be found which indicated that the graphite walls may not be strongly IR active as shown in Fig. 1A. For GO sample, the peak at 3404 cm^{-1} can be attributed to O–H stretching vibrations of absorbed water molecules and structural OH groups, and the peak at 1623 cm^{-1} can be attributed to O–H bending vibration [20]. After the HFTMS functionalization, these bonds were intact, and thus the corresponding peaks did not change significantly in either intensity or position. The presence of carboxyl functional groups in GO can also be detected at around 1746 cm^{-1} [20]. Its intensity decreased after HFTMS functionalization, indicating that carboxylic groups react with HFTMS molecules. The most significant change in FT-IR spectrum of GO-F was the large intensity decrease for peaks from ~2800 to ~3750 cm^{-1} , corresponding to the O–H stretching and deformation. This is due to the consumption of hydroxyl groups in GO sheets after hydrolysis with HFTMS. Upon further thermal treatment the remaining hydroxyl groups condense to loss water molecules and the intensity of O-H characteristic peaks decrease correspondingly.

XRD measurements were employed to investigate the crystalline of the synthesized hybrids. Fig. 2 depicts the XRD patterns of G, GO, GO-F and H-GO-F. While the characteristic peak corresponding to the (002) plane of pristine graphite appears at $2\theta = 26.67^\circ$, the GO pattern shows a strong peak at $2\theta = 10.14^\circ$, indicating the presence of oxygen containing functional groups after the oxidation process as shown in Fig. 2B [11]. After modification by HFTMS, a broad peak at $2\theta = 15^\circ\text{--}33^\circ$ can be found as shown in Fig. 2C. The drastic changes in GO and GO-F for the $2\theta = 15^\circ\text{--}33^\circ$ are due to the exfoliation of GO sheets after rapid vaporization of the intercalated water molecules. In particular, H-GO-F displays a stronger peak at $2\theta = 15^\circ\text{--}33^\circ$ and becomes broader after heat treatment which indicated that the interlayer distance d_{002} becomes larger. These XRD results are closely related to the exfoliation and reduction processes of GO and the processes of removing intercalated water molecules and the oxide groups of hydroxyl and carboxyl groups during the transition [21].

Fig. 3 shows the TGA curves for G, GO, GO-F and H-GO-F. Graphite shows a thermal stability up to 600 °C and a negligible weight loss, which is about 2% of its total weight in the entire temperature range. Comparing with the pristine graphite, GO shows the three weight loss stages. The first stage is around 120 °C, which results from the removal of adsorbed water. The second stage occurs at 200 °C due to the decomposition of labile oxygen-containing functional groups [14]. When the temperature was higher than 500 °C, GO decomposed rapidly and almost completely decomposed. The weight loss of GO-F dropped slowly in the entire temperature range in terms of desorption of water, physically bonded HFTMS, and chemically bonded HFTMS. However, in the case of H-GO-F, an enhanced thermal stability was observed for thermally treated sample with negligible weight loss below 300 °C. When the temperature was higher than 300 °C, H-GO-F decomposed rapidly due to the decomposition of covalently bonded HFTMS, together with the decomposition of GO.

After functionalization and thermal treatment, the resulting H-GO-F was dispersed in ethanol and filtrated to form a film. The surface morphologies of starting GO film, GO-F film and H-GO-F film are shown in Fig. 4. Compared with the starting GO film (Fig. 4A and B), the GO-F film exhibited an enhanced surface roughness (Fig. 4D and



Scheme 1. Structure change of GO in the HFTMS reaction and thermal treatment.

E). In the case of H-GO-F film, highest surface roughness consisted of many separated H-GO-F domains with flake dimensions ranging from several to tens of micrometers. The origin of the larger surface roughness of GO-F can be explained in terms of dispersion behaviors. The unmodified GO is well dispersed in ethanol, a polar solvent, leading to a slow vacuum filtration process. Thus, GO sheets form a well-stacked film with a smooth surface, which is thermodynamically stable [11]. However, for GO-F and thermally treated GO-F, their hydrophobic nature leads to poor dispersion in ethanol and the formation of aggregated domains. These large domains tend to be randomly oriented in the resulting film due to a fast solvent volatilization process. Thus, significant surface roughness can be produced, which is critical for fabricating superhydrophobic surfaces. Interestingly, in the case of H-GO-F film, the surface microstructure consists of ~ 5 nm-thick graphene sheets with a size of ~ 10 μm , as shown in Fig. 4H. To determine the superhydrophobicity of these films, water contact angle (WCA) measurements were performed at ambient conditions. The

starting GO film has the WCAs for a 5 μL water droplet with 37.5° and exhibited a hydrophilic surface, as shown in Fig. 4C. For the sample treated by HFTMS modification, the static WCA for 5 μL droplet was 106° which demonstrated an enhanced superhydrophobic surface (Fig. 4F). It is interesting to note that, the static WCA can be improved to more than 160° after the heat treatment (Fig. 4I). The microstructure and nanostructure provide sufficient roughness beneficial to surface hydrophobicity as described in Wenzel's theory [22]. Another important factor in surface property is surface free energy, which is highly relevant to the interior nature of graphene and the surface environment. As demonstrated above, the remaining labile oxygen-containing groups that are hydrophilic and physisorbed by HFTMS molecules can be removed after the thermal treatment. Compared to as-prepared GO-F, the surface energy of thermally treated GO-F film is further reduced. This implies that microstructure and interior nature governs and conveniently modulates the hydrophobicity of graphene films.

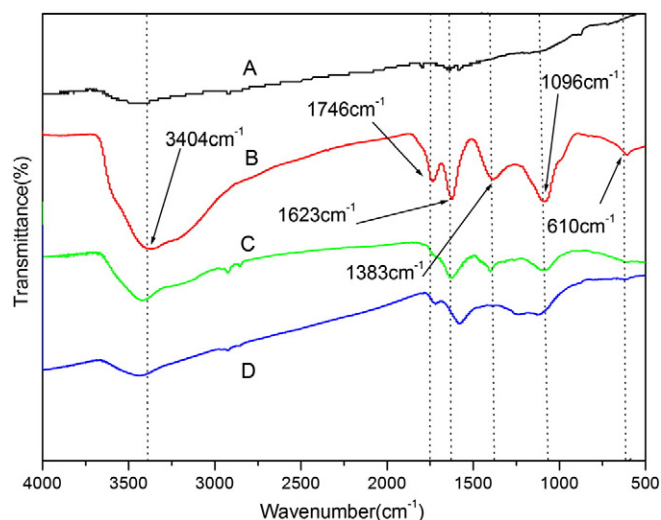


Fig. 1. FT-IR spectra of graphite (A), graphite oxide (GO, B), HFTMS modified GO (GO-F, C) and GO-F after heat treatment (H-GO-F, D).

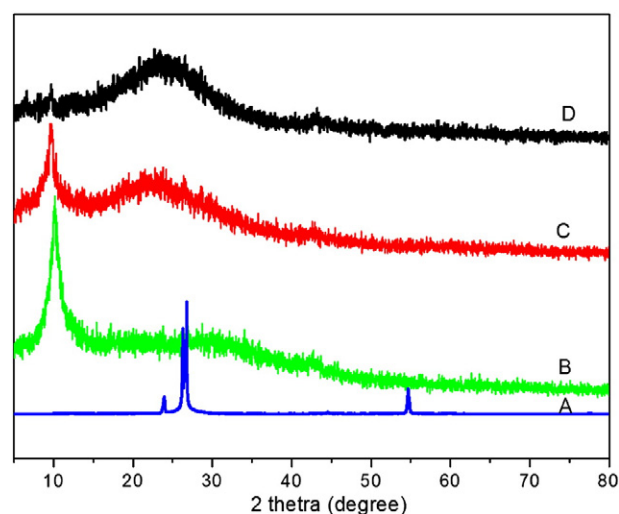


Fig. 2. XRD patterns of graphite (G, A), graphite oxide (GO, B), HFTMS modified GO (GO-F, C) and GO-F after heat treatment (H-GO-F, D).

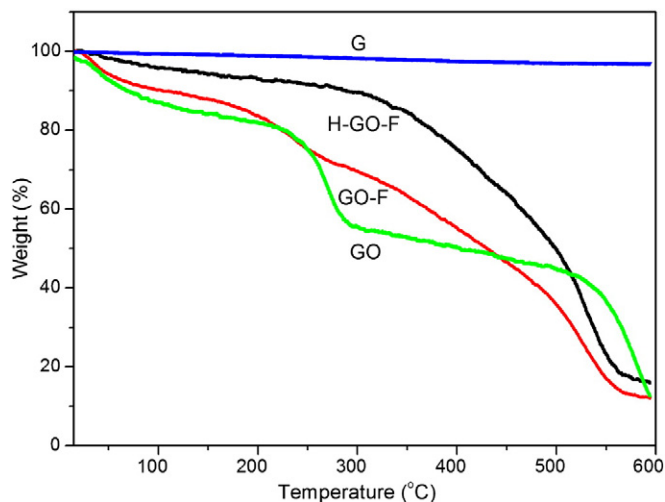


Fig. 3. TG curves of graphite (G), graphite oxide (GO), HFTMS modified GO (GO-F) and GO-F after heat treatment (H-GO-F).

To demonstrate the potential application of HFTMS modified GO in superhydrophobic coating, GO-F was dispersed in ethanol forming ~1.5 mg/mL dispersion. A thin GO-F coating on a glass substrate was

achieved using a drop coating method and heat treatment for 1 h at 150 °C. The optical image of a water droplet with 50 μ L on the surface of the as-prepared coating gives a direct demonstration of the superhydrophobic surface of functionalized graphene oxide films as shown in Fig. 5A. Whereas, coating surface can be absolutely wet by silicone oil and exhibited an oleophilic property. The superhydrophobic and superoleophilic surfaces may be used to separate oils from the water surface easily [23–25]. In another experiment, the platform was rotated to 180°, and the water droplet still can maintain its position without sliding and exhibited a good adhesive property, as shown in Fig. 5B. This phenomenon is similar to the nature of water drop on the leaves' surface. We believe that the HFTMS modified GO coated superhydrophobic surfaces can be achieved by various coating methods. Therefore, it is a practical material for low-cost and large-scale superhydrophobic coating.

4. Conclusion

Graphene films with high hydrophobic and adhesive performance were fabricated via chemical modification of graphite oxide and heat reduction processes. Irregularly stacked multilayer graphene nanosheets comprised the microstructure, whereas folding and agglomeration of graphene nanoflakes with few layers comprised the nanostructure. The films also showed remarkable superhydrophobic and oleophilic properties. On the other hand, the capillary force is maximized by the nanostructure such that water fills the grooves of the rough solid

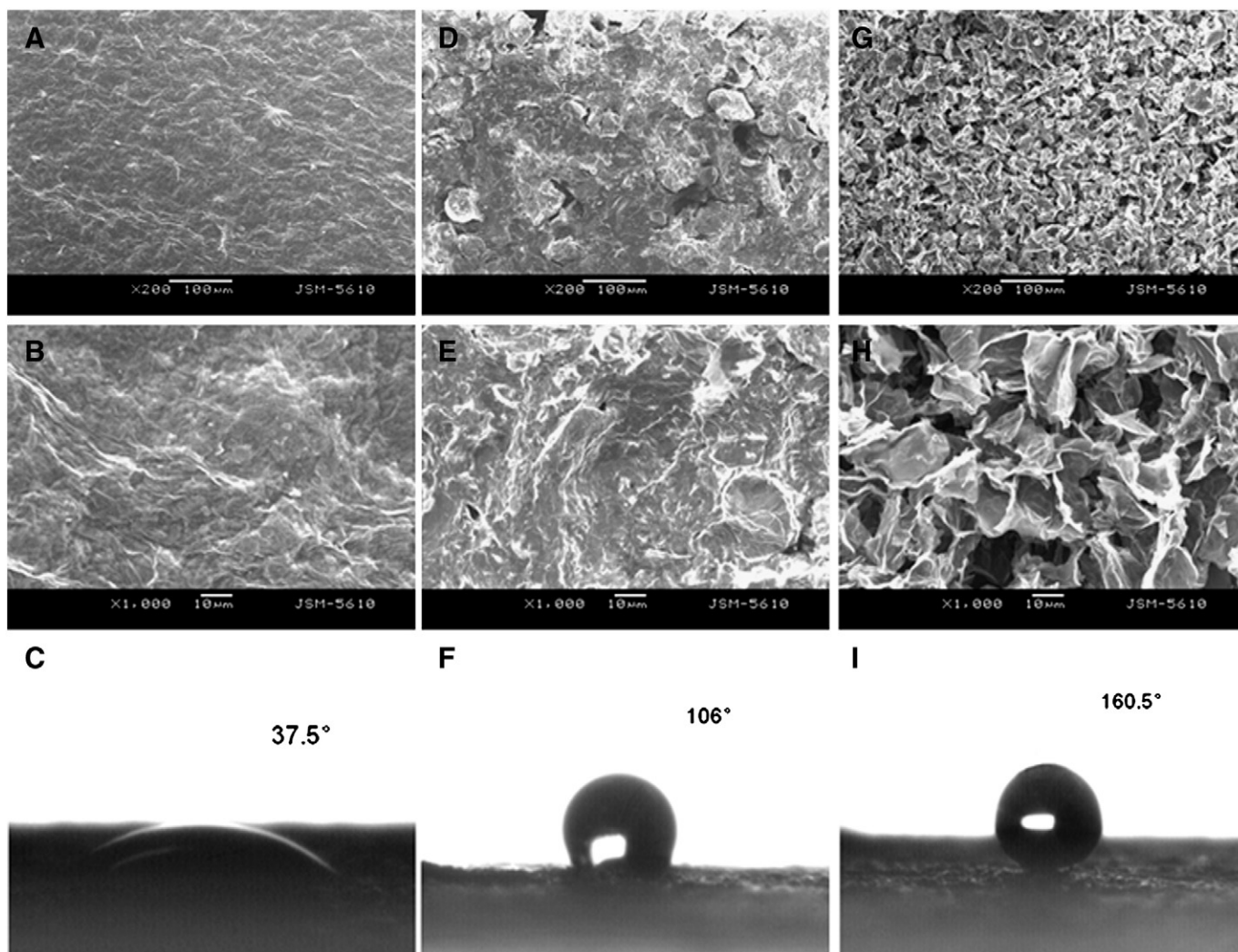


Fig. 4. SEM images with different magnifications and the water contact angles (WCA) with a 5 μ L water droplet of graphite oxide (GO, A, B and C), HFTMS modified GO (GO-F, D, E and F) and GO-F films after heat treatment (H-GO-F, G, H and I).

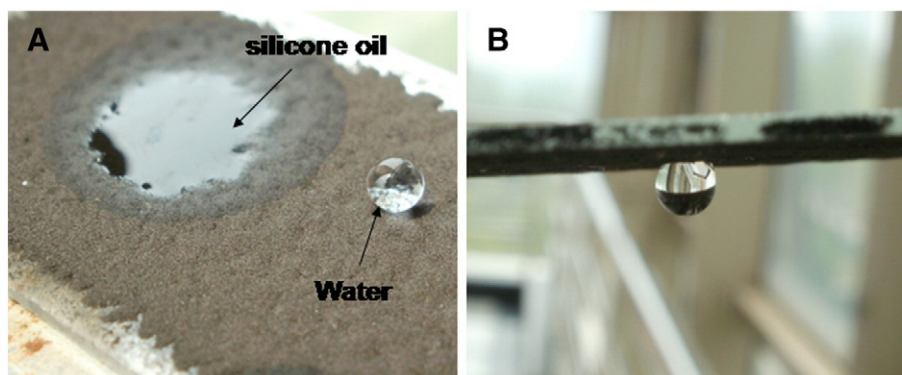


Fig. 5. Optical images of a 50 μL of silicone oil and water drop onto the HFTMS modified GO coating after heat treatment (A) and the water drop adhesive platform after it has been rotated to 180° (B).

surface. This results in a strong interaction between water and the film surface giving highly adhesive property to the films. The highly hydrophobic and adhesive performance of the graphene films could be useful in the device and biomaterial application.

Acknowledgments

This work was financially supported by the Qianjiang Talents Project of Zhejiang Province (2010R10023), the Scientific Research Foundation for the Returned Overseas Chinese Scholars, the State Education Ministry (1001603-C), the Natural Science Foundation of Zhejiang Province (Y4100045, R210154), Training Foundation for the Excellent Young Talents by the Key Laboratory of Advanced Textile Materials and Manufacturing Technology (ATMT), Ministry of Education (2011QN04) and the National Natural Science Foundation of China (51133006).

References

- [1] S. Garaj, W. Hubbard, A. Reina, J. Kong, D. Branton, J.A. Golovchenko, *Nature* 467 (2010) 190–193.
- [2] C.A. Merchant, K. Healy, M. Wanunu, V. Ray, N. Peterman, J. Bartel, M.D. Fischbein, K. Venta, Z.T. Luo, A.T.C. Johnson, M. Drndic, *Nano Letters* 10 (2010) 2915–2921.
- [3] T. Onda, S. Shibuichi, N. Satoh, K. Tsujii, *Langmuir* 22 (1996) 2125–2127.
- [4] M.C. Gordillo, J. Marti, *Physical Review* 78 (2008) 075432.
- [5] G. Wang, B. Wang, J. Park, J. Yang, X. Shen, J. Yao, *Carbon* 47 (2009) 68–72.
- [6] G.A. Kimmel, J. Matthiesen, M. Baer, C.J. Mundy, N.G. Petrik, R.S. Smith, Z. Dohnálek, B.D. Kay, *Journal of the American Chemical Society* 131 (2009) 12838–12844.
- [7] O. Leenaerts, B. Partoens, F.M. Peeters, *Physical Review* 79 (2009) 235440.
- [8] Y.J. Shin, Y.Y. Wang, H. Huang, G. Kalon, A.T.S. Wee, Z.X. Shen, C.S. Bhatia, H. Yang, *Langmuir* 26 (2010) 3798–3802.
- [9] X. Zhang, S. Wan, J. Pu, L. Wang, X. Liu, *Journal of Materials Chemistry* 21 (2011) 12251–12258.
- [10] J. Rafiee, M.A. Rafiee, Z.-Z. Yu, N. Koratkar, *Advanced Materials* 22 (2010) 2151–2154.
- [11] T.A. Pham, N.A. Kumar, Y.T. Jeong, *Synthetic Metals* 160 (2010) 2028–2036.
- [12] H.C. Schniepp, J.-L. Li, M.J. McAllister, H. Sai, M. Herrera-Alonso, D.H. Adamson, R.K. Prud'homme, R. Car, D.A. Saville, I.A. Aksay, *The Journal of Physical Chemistry* B 110 (2006) 8535–8539.
- [13] D. Pandey, R. Reifengerger, R. Piner, *Surface Science* 602 (2008) 1607–1613.
- [14] Z. Lin, Y. Liu, C. Wong, *Langmuir* 26 (2010) 16110–16114.
- [15] T. Szabo, O. Berkesi, P. Forgo, K. Josepovits, Y. Sanakis, D. Petridis, I. Dekany, *Chemistry of Materials* 18 (2006) 2740–2749.
- [16] P. Mukhopadhyay, R.K. Gupta, *Plastics Engineering* 67 (2011) 32–42.
- [17] G. Xue, H. Ishida, J.L. Koenig, *Angewandte Makromolekulare Chemie* 140 (1986) 127–134.
- [18] A.B. Bourlinos, D. Gournis, D. Petridis, T. Szabó, A. Szeri, Imre Dékány, *Langmuir* 19 (2003) 6050–6055.
- [19] B. Liu, L. Jiang, D. Zhu, *Advanced Materials* 14 (2002) 1857–1860.
- [20] P. Lian, X. Zhu, S. Liang, Z. Li, W. Yang, H. Wang, *Electrochimica Acta* 55 (2010) 3909–3914.
- [21] H.-M. Ju, S.-H. Choi, S.H. Huh, *Journal of the Korean Physical Society* 57 (2010) 1649–1652.
- [22] R.N. Wenzel, *Industrial and Engineering Chemistry* 28 (1936) 988–994.
- [23] Q. Zhu, Q. Pan, F. Liu, *Journal of Physical Chemistry C* 115 (2011) 17464–17470.
- [24] C.-W. Tu, C.-H. Tsai, C.-F. Wang, S.-W. Kuo, F.-C. Chang, *Macromolecular Rapid Communications* 28 (2007) 2262–2266.
- [25] T. Arbatan, X. Fang, W. Shen, *Chemical Engineering Journal* 166 (2011) 787–791.